Meteorol. Z. (Contrib. Atm. Sci.), Vol. **28**, No. 3, 235–253 (published online April 26, 2019)

Impact of DNI nowcasting on annual revenues of CSP plants for a time of delivery based feed in tariff

Jürgen Dersch[1], Marion Schroedter-Homscheidt[2], Kacem Gairaa[3], Natalie Hanrieder[4], Tomas Landelius[5], Magnus Lindskog[5], Stefan C. Müller[6], Lourdes Ramirez Santigosa[7], Tobias Sirch[8] and Stefan Wilbert[4]

[1]German Aerospace Center (DLR), Institute of Solar Research, Cologne, Germany
[2]German Aerospace Center (DLR), Institute of Networked Energy Systems, Oldenburg, Germany
[3]Unité de Recherche Appliquée en Énergies Renouvelables, URAER, Centre de Développement des Energies Renouvelables, CDER, Ghardaia, Algeria
[4]German Aerospace Center (DLR), Institute of Solar Research, Almeria, Spain
[5]Swedish Meteorological and Hydrological Institute (SMHI), Norrköping, Sweden
[6]Meteotest, Bern, Switzerland
[7]Ciemat, Dpto. de Energías Renovables, Madrid, Spain
[8]German Aerospace Center (DLR), Institute of Atmospheric Physics, Wessling, Germany

(Manuscript received May 16, 2018; in revised form March 4, 2019; accepted March 4, 2019)

Abstract

The impact of combined direct normal irradiation nowcasts on revenues of two different concentrating solar power plant technologies under a time-of-delivery tariff is investigated. The applied tariff scheme offers considerably increased remuneration during evening hours with maximum energy demand and is similar to that used in South Africa for some concentrating solar power (CSP) plants already. The ideal forecast derived from ground-based observations was used to quantify the maximum economic advantage of using any forecasting scheme - and is estimated around 4 % for parabolic trough power plants and as around 8 % for solar tower power plants. This implies a maximum impact of up to 2.2 Mio and 5.3 Mio EUR of additional revenues per year for a typical 110 MW solar trough or solar tower power plant, respectively. The investigated nowcast strategy merges several satellite and numerical weather prediction based nowcasts together with a smart persistence approach in order to generate a best-of nowcast for now- and forecast time horizons up to 9 hours and in the 15 min temporal resolution required for the electricity market participation. The results for the combined nowcast are evaluated with respect to daily power plant operating principles and focusing on a power plant specific forecast verification strategy. The combined nowcast is therefore compared with ECMWF IFS based forecasts and with an optimized ground observation driven persistence approach in two representative locations around the Mediterranean area. The study investigates the impact both with respect to annual energy yield and economic annual revenues of CSP plants. It is found that in our study period 2010 and 2013 to 2015 the merged nowcast strategy adds 0.8 to 4.4 % in additional revenues per year compared to the ECMWF IFS day ahead forecast, which is a typical example of nowadays routinely available forecasts in the power plant's control room. This implies additional revenues of about 450 to 2900 kEUR per year when adding a nowcasting scheme to the solar production forecast tool already in operation at some power plants.

Keywords: Concentrating solar power, direct normal irradiation, nowcasting, forecasting, operating scheme, revenues, dispatch optimization

1 Introduction

Concentrating solar power (CSP) plants with thermal storage are capable to deliver dispatchable solar electricity. This is a difference to solar photovoltaics (PV) and wind power plants which deliver fluctuating electricity if no batteries are used. Battery storage providing high power output for several hours in combination with PV or wind energy plants is currently more expensive than CSP with thermal storage (Lovegrove et al., 2018). In order to honor this additional value of CSP and to encourage higher solar electricity production during the peak evening hours, special tariff schemes are applied with varying remuneration depending on the time of delivery as e.g. the two-tier tariff in South Africa (Gauché et al., 2017). Under such economic conditions, plant owners will operate their plants in a manner which maximizes annual revenues rather than total electricity production. This requires an optimized strategy for storage and power block utilization. With time slots and feed-in tariffs set as fixed for these individual time slots by the market regulation scheme, the plant operators need to have a weather forecast in order to decide whether they shall use the solar heat immediately for electricity production or rather send it to the thermal storage and use it later when they may earn more money per unit. The lat-

*Corresponding author: German Aerospace Center (DLR), Institute of Solar Research, Linder Höhe, 51147 Köln, Germany, email: juergen.dersch@dlr.de

DOI 10.1127/metz/2019/0925

Gebrüder Borntraeger Science Publishers, Stuttgart, www.borntraeger-cramer.com

ter alternative implies the risk that they are going to lose money when the storage is completely charged already in the early afternoon hours while the direct normal irradiance (DNI) is still high. In this case they need to reduce the thermal output of the solar field by defocusing some heliostats or parabolic troughs since the solar field is typically capable to deliver solar heat in excess compared to the maximum heat input of the power block.

Concentrating solar power plants have started to use solar forecasting tools in recent years (e.g. Schroedter-Homscheidt et al., 2009 and Schroedter-Homscheidt and Pulvermüller, 2011; Kraas et al., 2013). They are mainly used for day-ahead forecasting of solar energy production for electricity trading and rely on numerical weather prediction either from global or mesoscale models. This study investigates the potential impact of extending these forecasting schemes by a nowcasting component. The first economic question raised by power plant owners is whether the potential impact of using an ideal nowcasting scheme is economically viable at all. This is the basis to invest any further research & development budgets to find the best nowadays available nowcasting strategy and provider. This study quantifies this potential impact by using the theoretical ideal nowcast as derived from ground-based observations as the observed truth, but used as a nowcast dataset in the power plant simulation.

Furthermore, this paper presents results from the EU FP7 research project DNICast (http://www.dnicast-project.net, accessed at 6.12.2018) evaluating a number of different nowcast strategies based on ground observations, meteorological satellites, numerical weather prediction (NWP) and combinations hereof. DNICast also applied cloud data assimilation in NWP models and coupling of satellites in the best member selection of mesoscale ensemble predictions. Based on these various approaches, a merger of nowcasts was developed to derive a best-of DNI nowcast and to couple the strengths of various methods in different forecast horizons. The impact of this best-of DNI nowcast on CSP plant revenues is investigated. This estimates the potential impact of a nowcasting scheme that can be reached with the nowadays state of the art in meteorological nowcasting.

Recently, papers on coupling CSP plant performance models with numerical optimization were published (Guedez et al., 2016, Wagner et al., 2017, Vasallo and Bravo, 2016). In Wittmann et al. (2011) dynamic programming is used to optimize the revenues in a liberated electricity market with varying prices. These authors did not consider DNI forecasts and their impact on revenues which is the main goal of this paper. Kraas et al. (2013) used DNI forecasts based on model output statistics for the day-ahead time range of +24 to +48 hours in hourly temporal resolution. They quantified the impact on the day-ahead market participation use case and how much penalties for schedule errors can be avoided by good forecasts. Do Amaral Burghi et al. (2017) presented a heuristic method combined with probabilistic day-ahead DNI forecasts in a fixed revenue scheme and penalties for under-fulfilling the originally scheduled production. They did not use any nowcasting scheme in combination with the day-ahead forecasts.

This paper is organized in the following manner: Section 2 introduces the validation data as well as the nowcasts and forecasts used in the study. Section 3 describes the tariff scheme and the revenue quantification depending on various operating strategies for such power plants. Section 4 presents results for two locations and various years and for both solar tower and trough plants, before Section 5 concludes the paper.

2 Data

Two sites are considered in this study: Plataforma Solar de Almeria (PSA, 37.091° N, −2.3° W, 492 m amsl) in Spain and Ghardaia (GHA, 32.386° N, 3.780° E, 463 m amsl) in Algeria. They were selected as representative locations for the CSP sector but also as providing different climatic conditions in Southern Spain and in Northern Africa. Please note that the power plant simulation done in the study assumes a typical CSP power plant located at these two locations, but does not simulate real existing power plants. This is a restriction typical in an industrial environment where any ground-based observations at an existing power plant site are not available for research projects as they are classified as company confidential information by the power plant owner.

2.1 Ground observations

Only ground-based observations providing the direct and the global component are of interest. Direct irradiance measurements are highly sensitive to daily cleaning of the sensors and require a rigorous data quality control. Therefore, the study focuses on high quality measurements obtained by DLR at the PSA test site in Southern Spain and the station GHA being part of the EnerMENA meteorological network in the MENA (Middle East and Northern Africa) region (Schüler et al., 2016).

The ground measurement program ‘enerMENA meteo network’ applies ventilated CMP21 Secondary Standard Kipp & Zonen pyranometers and Kipp & Zonen CHP1 First Class pyrheliometer instruments as well as rotating shadow band irradiometers at various locations in Algeria, Egypt, Jordan, Morocco and Tunisia. In GHA the mentioned thermopile radiometers are used.

The PSA data provides 1-min measurements obtained with First Class pyrheliometers (ISO 9060, 1990) and Secondary Standard pyranometers (ISO 9060, 1990) mounted on a solar tracker with sun sensor. Further information in the instrumentation can be found in Wilbert et al. (2013) for PSA and in Schüler et al. (2016) for GHA.

This data is quality controlled following the method from Geuder et al., 2015. The method is based on recommendations of the MESOR project (Management

and Exploitation of Solar Resource Knowledge, Beyer et al., 2008) which is an extension to the BSRN (Baseline Surface Radiation Network) quality control standards (as published originally in internal BSRN documents and later in peer review by Long and Dutton, 2012) with special focus on the solar energy sector. In addition to the automatic filters for the irradiance and other meteorological parameters the quality control also included the manual visual control by a scientist.

Wind direction and speed measurements at 10 m height, atmospheric pressure and temperature and relative humidity measurements at 2 m height complement the radiation data. These measured data sets are used for all simulations as if perfect forecasts of these parameters would be available in order to focus the study only on the effect of the DNI forecast.

2.2 Forecast datasets

For the study 5 different fore- and nowcasts datasets are used for both power plant locations under investigation. They are selected with the following rationale:

- The Day 1 ECMWF (European Centre for Medium-Range Weather Forecasts) forecast is available at about 8:00 UTC and is valid for the day ahead (+24 to +48 hours forecast horizon). This forecast is nowadays already available at the power plant control room for the day-ahead forecast. Using this forecast would be possible without extra costs for the power plant owner. Therefore, it is selected as the reference to quantify the economic impact of any other scheme which at the end has to be compared versus additional costs in a cost-benefit analysis.
- The Day 0 ECMWF forecast is available at the current day at about 8:00 UTC and is valid for the actual day (up to +24 hours forecast horizon).This forecast is nowadays not available at the power plant control room as it is not provided early enough during the day for the day-ahead use case already. But it may be added as nowcasting option with rather low costs as the data flow itself to the ECMWF forecast data provider is established already.
- Persistence forecast based on DNI ground-based measurements with a refresh rate of 15 minutes. This is a solution with additional costs for the power plant owner as ground-based measurements need to be maintained with a daily cleaning and an extra data flow needs to be implemented and quality controlled. Therefore, persistence is not suitable as the reference in our case, but it may be a cheaper solution than purchasing a nowcast as addition to the already available day-ahead NWP based forecast.
- DNICast combined forecast with a refresh rate of 15 minutes. This is a newly developed nowcasting making use of various nowcasting methods (see below)
- Ideal forecast generated from DNI ground-based measurements. This is an optimum forecast without any forecast error. It results in the maximum revenues which can be reached by the power plant and a specific operating strategy. It is used to estimate the maximum positive impact any perfect nowcast scheme may have. It defines the upper range of any procurement costs an industrial user will be willing to pay for any nowcast scheme.

ECMWF forecasts are obtained from the deterministic Integrated Forecast System (IFS) model run started at 00 UTC. In this study, only the 0 UTC ECMWF run was used. The 12 UTC run is available only too late to be useful for this application of a ToD tariff with a peak demand in afternoon/early evening hours as forecast priority.

For the location PSA, forecasts from 2010, 2013, 2014, and 2015 are used, while for GHA only the years 2013 and 2014 are available as ground observations. IFS forecasts are obtained on a regular 0.15° latitude and longitude grid as being operated for the time period under investigation. Afterwards, forecasts are interpolated bi-linearly to the location of interest. Three-hourly integrated solar surface downward radiation (SSRD) is interpolated to 1 min resolved forecasts by taking the solar daily cycle and the actual atmospheric turbidity into account. The clearness index as ratio of the forecasted irradiation versus the extra-terrestrial irradiation is used to interpolate first in the 'clearness index space' over time and afterwards the 1 min resolved forecast is derived from the astronomically well-defined 1 min resolved extra-terrestrial irradiation.

The persistence forecast uses the 1 min resolved DNI measurement from a pyrheliometer as input for PSA. For GHA, 10 min resolved DNI measurement data have been interpolated linearly to 1 min resolution. Firstly, the Linke turbidity is calculated for the last timestamp with a DNI measurement of this station using the Linke turbidity model from Ineichen and Perez (2002). Together with the air mass of future timestamps, this Linke turbidity is used to derive the DNI using again the model from Ineichen and Perez (2002). This DNI is used as the persistence forecast (named 'persistence' below).

The DNICast combined forecast ($DNI_{combined}$) is based on the uncertainty weighted combination approach of Meyer et al. (2008). Separately run nowcasts, namely two satellite and two numerical weather prediction (NWP) based nowcasts, as well as the persistence nowcast are included in the combination.

The two satellite based nowcasts make both use of Meteosat Second Generation (MSG) SEVIRI imagery and include an optical flow cloud motion vector technique (Sirch et al., 2017; indicated as 'optical flow' below) and a sectoral cloud motion vector technique (Schroedter-Homscheidt and Gesell, 2016; indicated as 'receptor' below). The method of Sirch et al. (2017) couples the thin ice cloud detection method COCS (Kox et al., 2014) with the liquid water cloud and

Table 1: Naming of the different NWP+CI datasets.

Dataset	Aerosol Input	DNI method	Clear sky model
NWP+CI, clim	Climatology	indirect	ESRA
NWP+CI, climdirect	Climatology	direct	ESRA
NWP+CI, maccdirect	MACC	direct	Simple Solis

thick cirrus cloud detection method APICS (Bugliaro et al., 2011). With help of the Cb-TRAM algorithm for handling of quickly developing convective clouds and especially for tracking their pixel-wise motion vector field (Zinner et al., 2008 and 2013; Merk and Zinner, 2013) the movement of individual cloud objects is predicted. Quickly thinning convective clouds are treated separately to describe their dynamic behavior. Finally, radiation is derived from cloud optical thickness and the Lambert-Beer law. The method was extensively validated in Sirch et al. (2017) resulting in accuracy estimates used as statistical weights in the $\text{DNICast}_{\text{combined}}$ merger approach.

The method of Schroedter-Homscheidt and Gesell (2016) uses the cloud retrieval package APOLLO (Saunders and Kriebel, 1988; Kriebel et al., 1989; Gesell, 1989; Kriebel et al., 2003) to separately derive cloud masks and physical properties of thin cirrus and optically thick cirrus and/or water clouds. A receptor model tracks cloud objects coming towards the power plant's location from 32 individual sectors. Cloud objects are separated between thin cirrus clouds and other clouds as they often show different movement directions and speed. An ensemble of cloud optical thickness estimates is set up using all pixels of a cloud object within the relevant sector from where the cloud reaches the power plant. Based on this spatial ensemble a probabilistic range of cloud optical thickness and – with the help of the Lambert-Beer relationship – the DNI is estimated. This DNI range is interpreted in the merger as an uncertainty estimate quantified for each nowcast individually based on the actual atmospheric conditions.

In addition to the satellite-based nowcasting, newly developed NWP based approaches were used. Clear sky satellite radiances from the two MSG SEVIRI channels (at 6.25 and 7.35 µm) that are sensitive to water-vapor were assimilated together with conventional observations into an experimental run of the regional NWP model HARMONIE/AROME using 4D-Var (Landelius et al., 2016, indicated as 'SMHI NWP 1' below, available only for April 2013). Cloud masks and physical properties as cloud top temperature and cloud base height are derived from EUMETSAT Satellite Application Facility for NoWCasting & Very Short Range Forecasting (SAFNWC) software for the MSG SEVIRI imagery (Le Gleau and Derrien, 2002). In a second experiment (indicated as 'SMHI NWP 2' below) they were used in the HARMONIE-AROME model (Bengtsson et al., 2017) by using an innovative cloud initialization procedure based on van der Veen (2013) followed by 3D-Var assimilation of conventional observations. In this experiment the satellite radiance were not assimilated directly. Instead the SAFNWC cloud products that are derived from the radiances were used. Not only the model cloud fields, but also the temperature and humidity fields are modified. Validation results of this individual method are provided in Landelius et al. as chapter 1 in Gaston et al., 2017.

In a second NWP based approach nowcasts are based on a combination of mesoscale model wind fields from WRF and MSG SEVIRI based clearness index (CI) fields are used (Müller et al. as chapter 1 in Landelius et al., 2016; named 'NWP+CI' below). The High Resolution Visible (HRV) channel is used to derive clearness index values as the ratio between cloudy sky irradiances and the clear sky irradiance. These CI values are propagated with WRF based wind trajectories for the next 4 hours before calculating DNI. Different approaches to calculate the DNI using different aerosol input (climatology or real-time MACC data) and indirect conversion from CI to GHI to DNI or direct conversion from CI to DNI by following Hammer et al. (2009). Details on the WRF model configurations and the solar radiation modelling are given in Landelius et al. (2016). The datasets are named according aerosol (climate/MACC) input and direct/indirect approach for DNI calculation (see Table 1).

$\text{DNI}_{\text{combined}}$ is computed from all available nowcasted DNI_i of the according data set i for each set of refresh time and forecast time:

$$\text{DNI}_{\text{combined}} = \left(\frac{1}{\sum_{i=1}^{n} \frac{1}{\Delta i}} \right) \cdot \left(\sum_{i=1}^{n} \frac{\text{DNI}_i}{\Delta i} \right)$$

Δi is the absolute error for each data set i per time stamp. Δi is provided for each data set within the DNICast project by the nowcast provider – either based on statistical assumptions originating from previously made evaluations against ground observations or based on an ensemble approach providing percentiles as an online accessible nowcast accuracy estimate valid for the individual nowcast. $\text{DNI}_{\text{combined}}$ is provided in a refresh interval of 15 minutes, with a temporal resolution of 15 minutes and for a horizon of 9 hours. All input nowcasts provide different refresh intervals, temporal resolutions, and forecast horizons (Table 2). They were individually validated in Dubranna and Saint-Drenan (2017) with strongly varying results for various stations/regions and nowcast methods and without any method performing best at the majority of locations. This motivated the approach chosen in this study to create a best-of combination based on the nowadays available state of the art

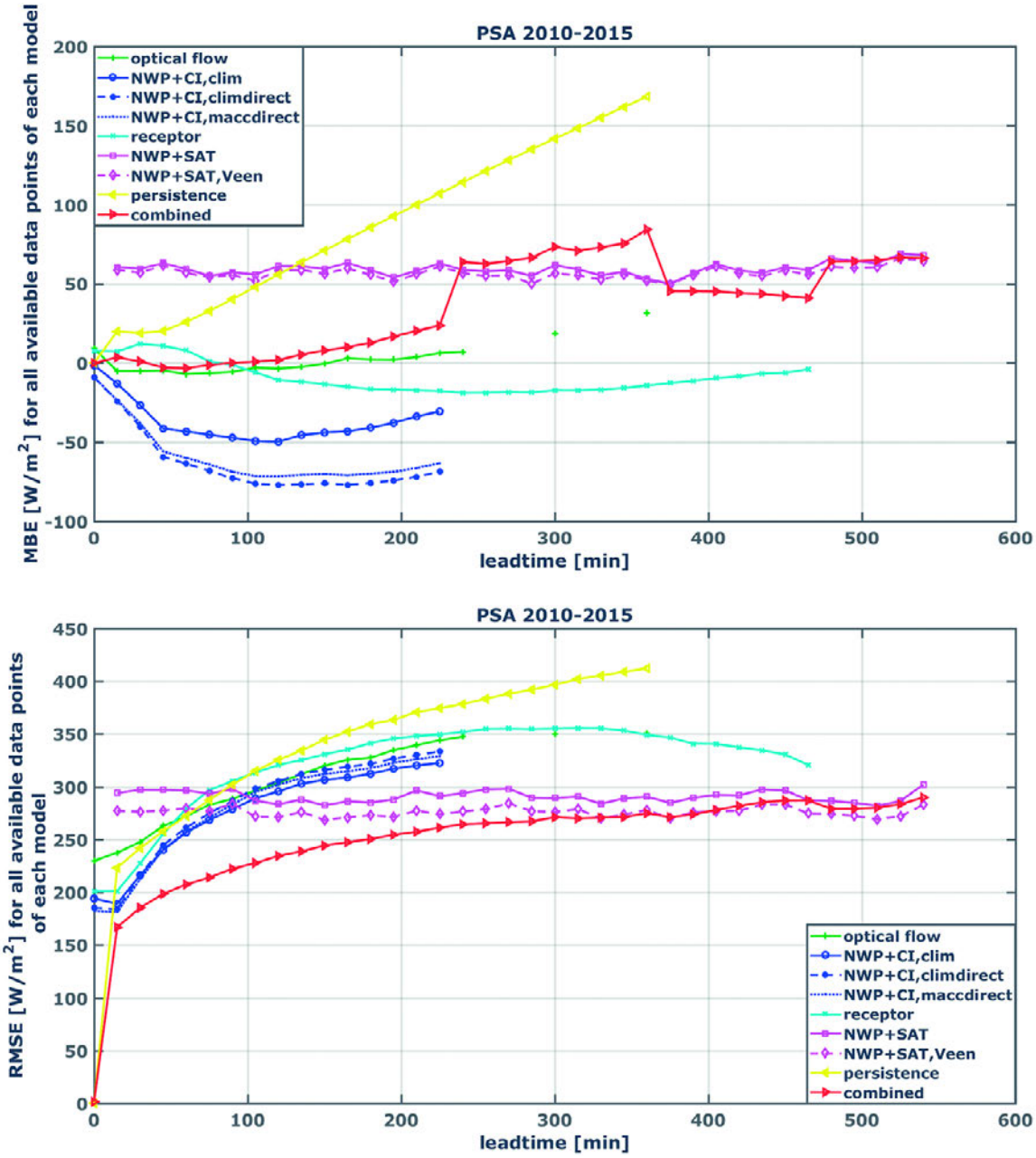

Figure 1: Absolute MBE and RMSE for all available data points for each individual nowcasts and the combined nowcasts for PSA.

Table 2: Main characteristics of the available nowcast methods used as input for DNIcombined.

Dataset	Refresh interval (min)	Time res. (min)	Horizon (hour)
receptor	15	1	8
Optical flow	15	5	6
NWP+CI, various	15	5	4
NWP+SAT	180	15	9
NWP+SAT,Veen	180	15	9

and for the time of the study to exclude the question for the best performing stand-alone algorithm.

The performance of DNIcombined versus on-site DNI measurements from PSA and GHA stations was evaluated. Mean biased errors (MBE) of 0 to about 8 W/m^2 and mean root mean square errors (RMSE) from 0 to about 290 W/m^2 are found for 0 minutes to 9 hours lead time for PSA (for GHA MBEs between 8 and 123 W/m^2 and RMSE from 63 to 273 W/m^2, respectively, see Fig. 1 and Fig. 3). Relative MBEs lie between −0.006 and 0.17 and relative RMSEs between 0 and 0.58, as shown in Fig. 2 and Fig. 4 (MBEs between 0.02 and 0.24 and RMSEs between 0.12 and 0.53 for GHA, respectively). DNIcombined outperforms all individual nowcasts for lead times larger 15 minutes in terms of absolute RMSE. Fig. 1 and Fig. 3 provide both absolute MBE and RMSE for PSA and GHA stations for all available data points for each individual nowcast and the combined nowcast. All available data points imply that there is a different number of data points for

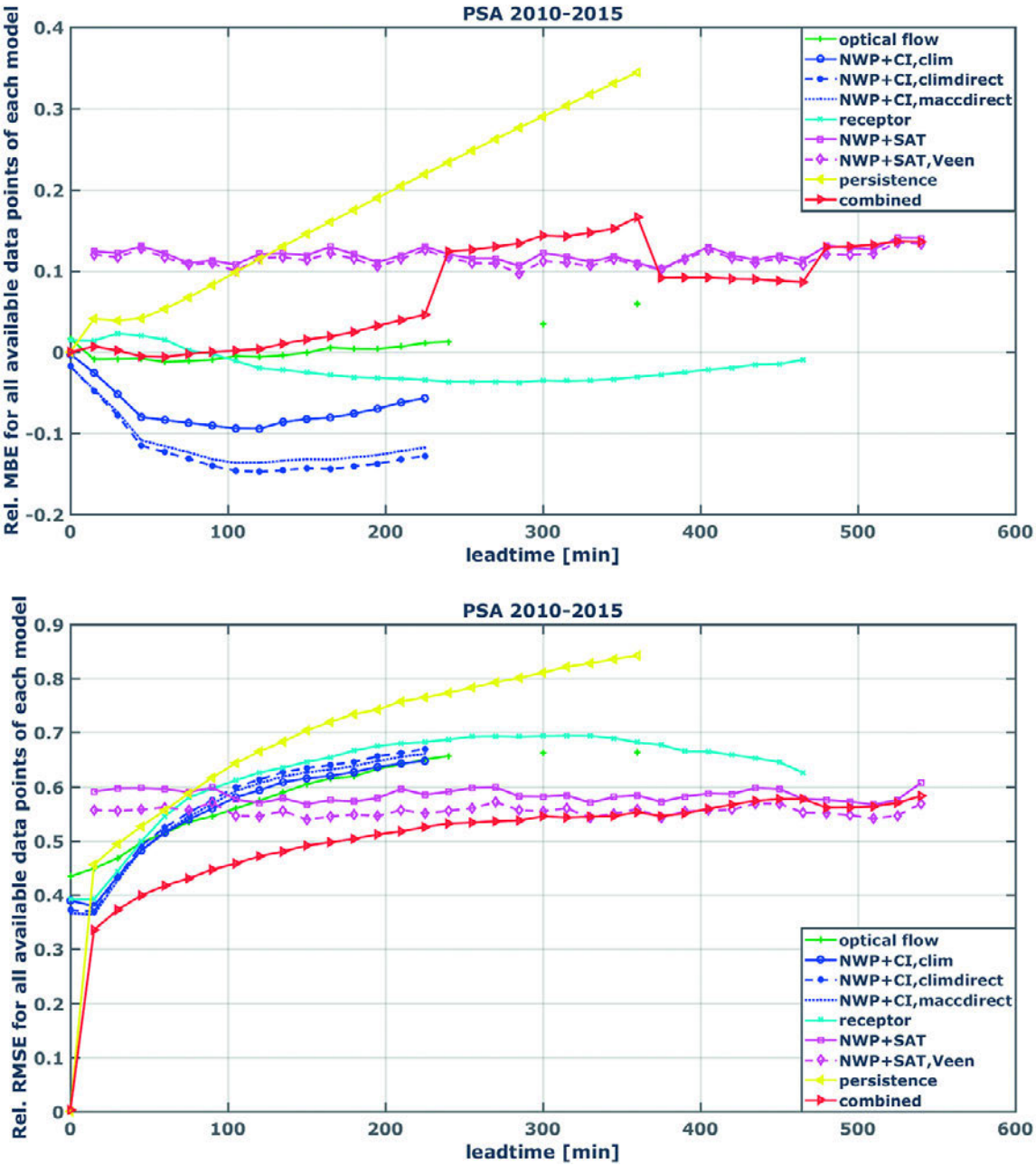

Figure 2: Relative MBE and RMSE for all available data points for each individual nowcasts and the combined nowcasts for PSA.

each method, as they have different temporal resolutions and forecast horizons each. These evaluations include all available nowcast periods which sums up to 12 months for PSA in 2010, and 2013 to 2015 and 6 months for GHA in 2013 – 2014. The number of available evaluated data points for each method is shown in Fig. 5. Note, that especially the methods NWP+SAT and NWP+SAT,Veen were available only for April 2013 as they originate from a short experimental run. All other methods were available for all months evaluated.

The analysis shows that for the PSA location the MBE of $DNI_{combined}$ set lies in between up to lead times smaller than 225 minutes. For these lead times, three data sets show a negative MBE (NWP+CI, clim, climdirect and maccdirect), while three data sets display a rather positive MBE (NWP+SAT and NWP+SAT, Veen and persistence). For higher lead times, the NWP+CI nowcasts are not available anymore, therefore a shift of the MBE for the combined nowcasts to higher MBEs can be observed. The RMSE of the combined data set is smaller for lead times below 300 minutes and approaches to the NWP+SAT and NWP+SAT,Veen values as the best performing nowcast for more than 300 minutes.

For GHA, both MBE and RMSE are in general similar as for PSA, but the persistence nowcasts performs in total better as only 6 and not 12 months have been analysed, not considering the autumn and winter months of January, February, March, September, October and November where the probability of cloudy conditions

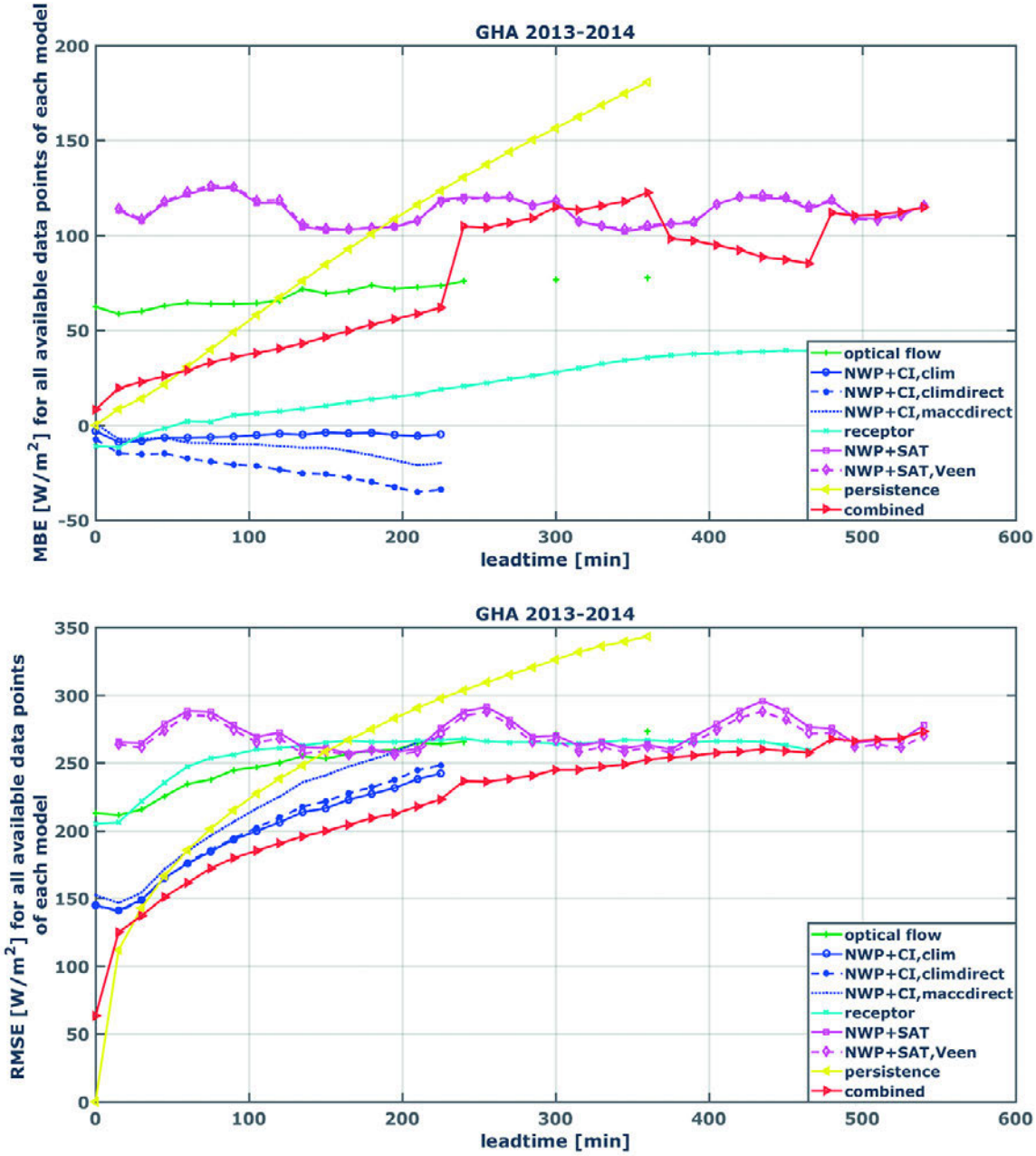

Figure 3: Absolute MBE and RMSE for all available data points for each individual nowcasts and the combined nowcasts for GHA.

is usually larger. The NWP+SAT and NWP+SAT, Veen nowcasts show higher MBE than for PSA which also increases the MBE of the combined nowcast.

2.3 Study period and gap filling

$DNI_{combined}$ is provided for the two sites and six time periods of three months duration each (PSA: Jan–Mar 2010, Mar–May 2013, Jun–Aug 2014, Sep–Nov 2015; GHA: Mar–May 2013, Jun–Aug 2014). The assessment of several years is necessary to avoid any specific year which is known in solar energy to be very unfortunate, as weather conditions heavily vary from year to year. On the other hand, processing time restrictions for some of the nowcasts occurred in the DNICast project. This is caused namely by methods applying very computer intensive ensemble predictions, high resolution mesoscale modeling for large areas as the Iberian Peninsula, or cloud data assimilation schemes into mesoscale models with a large spatial coverage from Iberian Peninsula to Northern Africa. As a compromise several years were treated, but with only 3 months periods each. These 3 months periods were selected due to ground observation data availability and by ensuring large cloud type variability. This was confirmed with the help of cloud statistics (Wey and Schroedter-Homscheidt, 2014) based on 2004 to 2015 cloud physical parameters as retrieved from Meteosat Second Generation satellite imagery.

The software Greenius (Dersch and Dieckmann, 2015; Dersch et al., 2010; http://freegreenius.dlr.de,

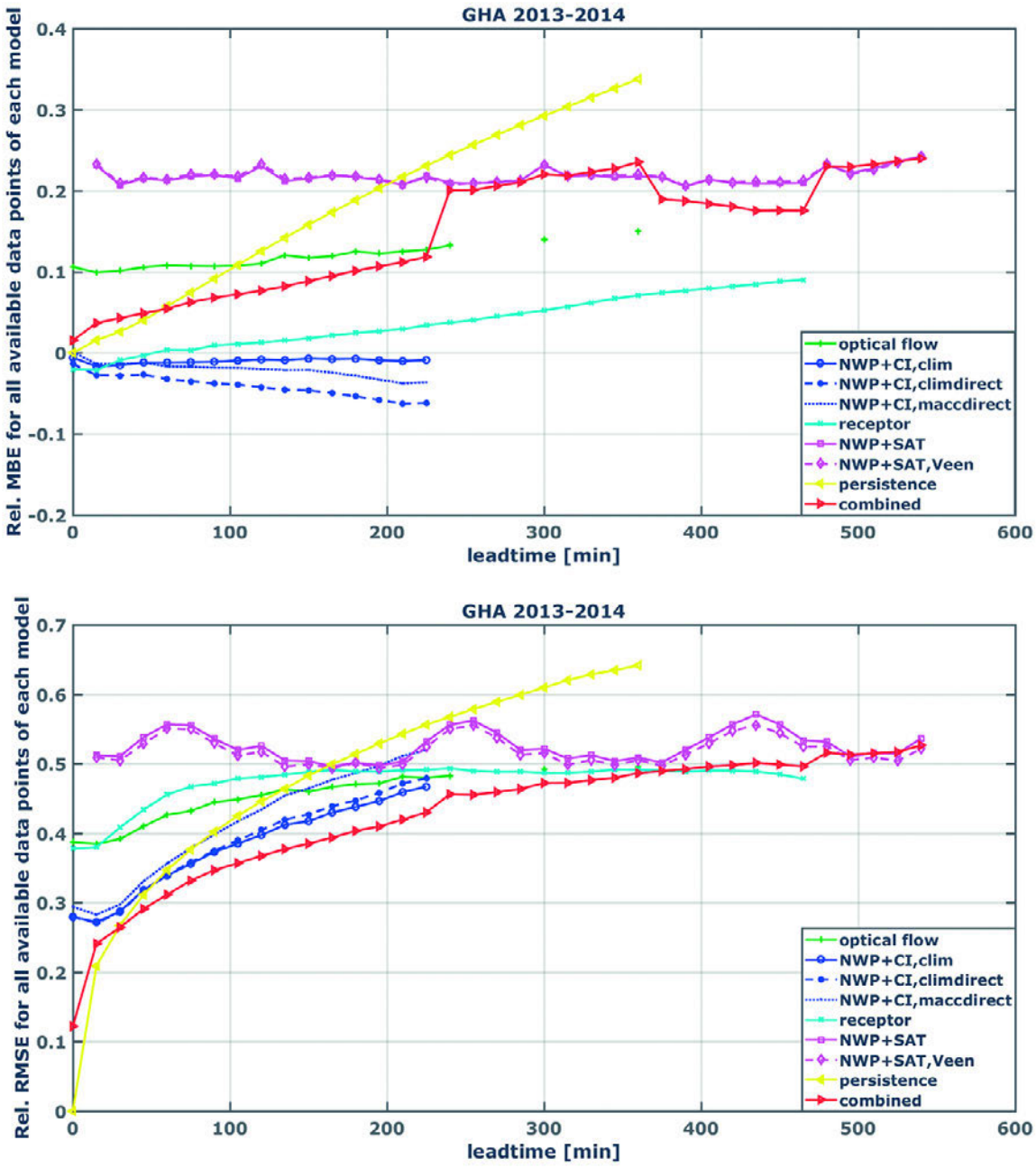

Figure 4: Relative MBE and RMSE for all available data points for each individual nowcasts and the combined nowcasts for GHA.

2018) as existing state-of-the-art CSP plant model, is used in this study to evaluate the impact of different forecast datasets. As Greenius is made for the simulation of a full year, the remaining hours of the year are filled up with the ECMWF day0 dataset as a forecast being available to the power plant operators easily as alternative. This is also valid for the persistence forecast dataset which was also only generated for the test periods in the DNICast project. So, any positive impact observed in our study by using only 3 months of a potentially better nowcast scheme (either based on persistence or the combined method) provides a minimum estimate of the impact expected for the full operations of such a scheme. This is a restriction of this study, but well justified as it allows to make use of very recent developments in the meteorological sector which are still needing large computing facilities for such experimental runs.

2.4 Other meteorological parameters

Additionally, ambient temperatures and wind speed data are always taken from the ground-based measurements as there are no nowcasts for these parameters available from all methods. Their impact on plant output is more than one order of magnitude lower than the DNI (Chhatbar and Meyer, 2011).

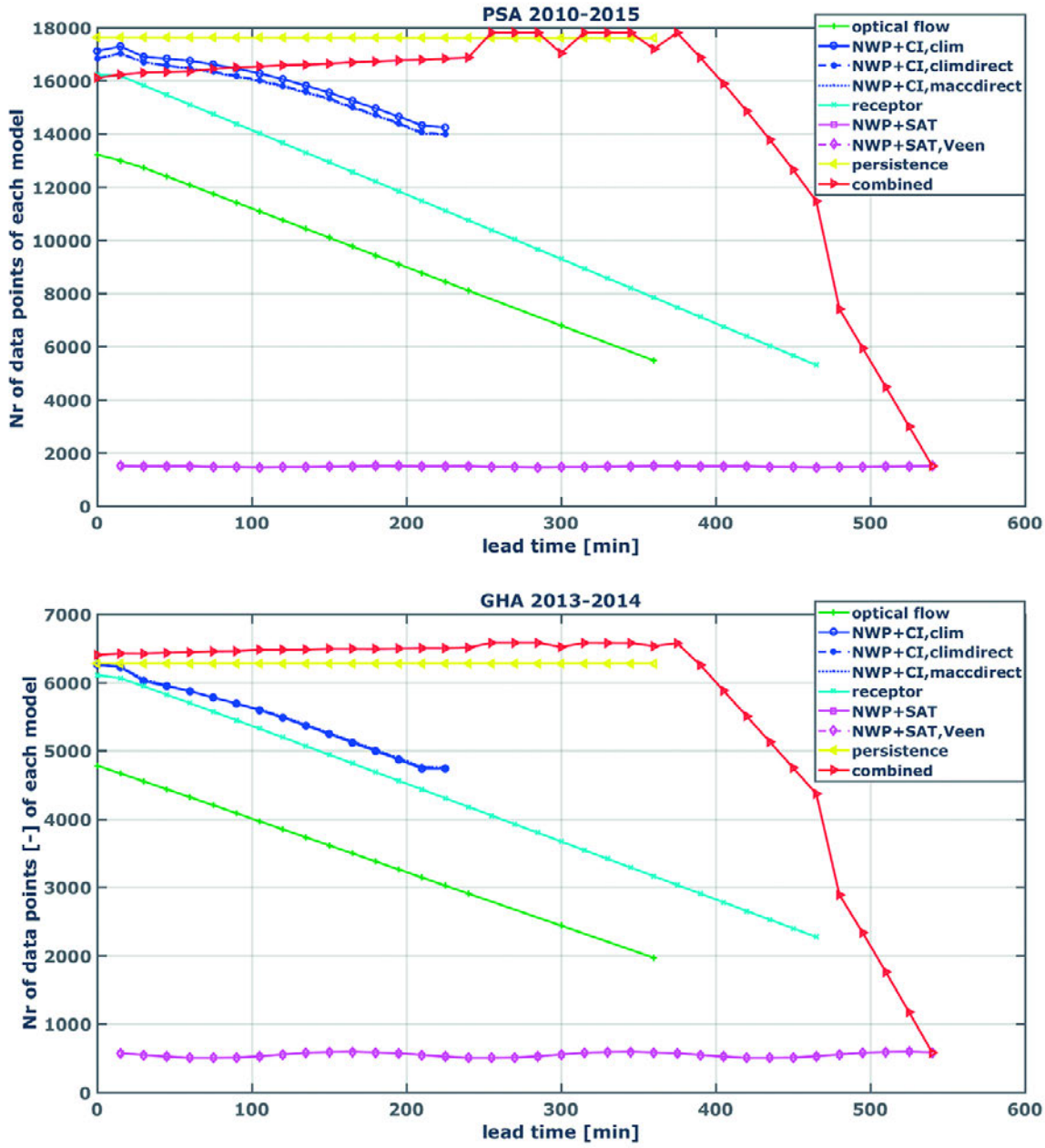

Figure 5: Number of available evaluated data points for each nowcast method for PSA and GHA.

3 Method

3.1 Tariff scheme

Any kind of flat tariff with constant remuneration will not be a big challenge for plant operators regarding an optimization of revenues. In contrast, a time of delivery (ToD) tariff with different remuneration rates for different hours of the day will require an optimized strategy for storage and power block utilization. The ToD tariff assumed here has a nominal feed-in tariff for every kWh delivered between 5:00 and 16:30 as well as between 21:30 and 22:00 (Fig. 6). All times mentioned in this paper refer to the local time at the site since this is relevant for the tariff. For the electricity delivered between 16:30 and 21:30 the remuneration is 2.7 times of the nominal feed-in tariff and for the remaining night hours there will be no remuneration at all. This scheme is derived from the two-tier tariff in South Africa (Gauche et al., 2017). It can be expected that the impact of nowcasting will be more pronounced in the case of such a ToD tariff as a nowcasting scheme allows a shift of storage-based electricity production to peak hours. Such a ToD tariff also means that the levelized cost of electricity which is often used as figure of merit for CSP systems is no longer the target for optimization. Owners are rather interested in maximizing their revenues. As a side effect the results of this study are not depending on cost assumptions for erection, operation and maintenance of the CSP plants since these assumptions are not needed for the calculation of revenues.

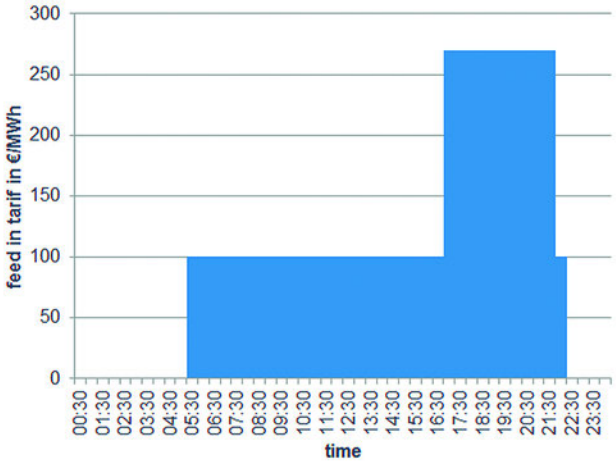

Figure 6: Time-of-Delivery tariff scheme used in this study.

3.2 CSP plant model

The annual yield simulation tool Greenius (Dersch et al., 2010; http://freegreenius.dlr.de) is used to calculate the annual output of two different CSP plants under the same boundary conditions. While the parabolic trough plant uses thermal oil as heat transfer fluid, the solar tower is simulated as using molten salt as heat transfer fluid. Both CSP plants are equipped with molten salt thermal storage for five hours of full load power block operation since this allows dispatching the electricity production. The nominal gross electrical output of both plants is 110 MW. Further technical details of the plant configurations are given in Annex A. Originally, Greenius was made for the simulation of CSP plants using DNI, ambient temperature, and wind speed data of a typical meteorological year as input. The temporal resolution of this typical meteorological dataset should be 1 hour or finer, depending on the model time step.

The CSP plant needs to be specified especially in terms of collector type, solar field reflective aperture, collector arrangement, thermal storage size, power block size, and performance data. Physical and empirical equations are used to calculate the output of the solar field and the whole CSP plant with the storage facility - based on the meteorological dataset and with the same temporal resolution as given in the meteorological dataset. Fig. 7 shows the overall program structure of Greenius. This software also allows for user defined operating strategies in order to adapt the electricity production to a specific demand structure. The final result contains the performance of the CSP plant for each time step given in the meteorological dataset including the net electricity production. This production is multiplied by the tariff for each time step and summed up to calculate annual revenues for the CSP plant.

In this study 15 minutes are used as temporal time step for both simulation and meteorological data. All meteorological input datasets are interpreted as mean values of the interval before the current time stamp. The existing version of Greenius was already capable to consider different operating strategies based on user defined rules like limits of power block load for individual time steps or minimum thermal storage charge state as precondition for power block operation, etc. But it was not made for adapting the operation strategy to frequently updated DNI forecasts while the simulation is running. Therefore it was modified to quantify the expected solar field output for the remaining time steps of the current day by using any updated forecast dataset. So, the modified Greenius version calculates the current time step and additionally all remaining time steps of the current day in order to predict the solar heat production for this day. Based on this information the operating strategy is updated as soon as a new nowcast is available.

3.3 Economic decision tree

Generally, in case of a flat or constant feed-in tariff a "solar-only" operating strategy (OS) would rather be used, which is characterized by the priority to operate the power block at maximum possible load whenever solar heat is available from the solar field. If the solar field output exceeds the maximum possible input to the power block, the excess heat is used to charge the storage. When the heat from the solar field is not sufficient to run the power block at nominal load, it is supplemented or completely replaced by discharging the storage. This solar only OS will give the highest annual electricity production since the power block is running under nominal load for most of the time and losses caused by defocusing are minimized.

The goal under a ToD tariff is always to produce as much electricity as possible during peak tariff hours to maximize annual revenues, rather than to reach the maximum annual electricity production. Together with the current storage charge state the projected solar field production is used to calculate the projected electricity production for the current day (Fig. 8). The decision whether to use the heat production immediately to produce electricity or rather send it to the storage is mainly made by comparing this projected electricity production to the maximum production for the day with some additional constraints (e.g. storage content, minimal power block load). A similar decision is made concerning the utilization of heat from the thermal energy storage (TES) to operate the power block or not. The path on the right hand side in Fig. 8 is only relevant when the heat delivered by the solar field is not sufficient to operate the power block at maximum load. During a single time step there is either storage charging or discharging, each of these modes excludes the other one. The method used here is therefore a heuristic one in contrast to a full optimization, but for this problem it is considered as appropriate as discussed in Chapter 4. The remaining heat demand and production for the current day are recalculated every time step and the decisions are checked and eventually revised.

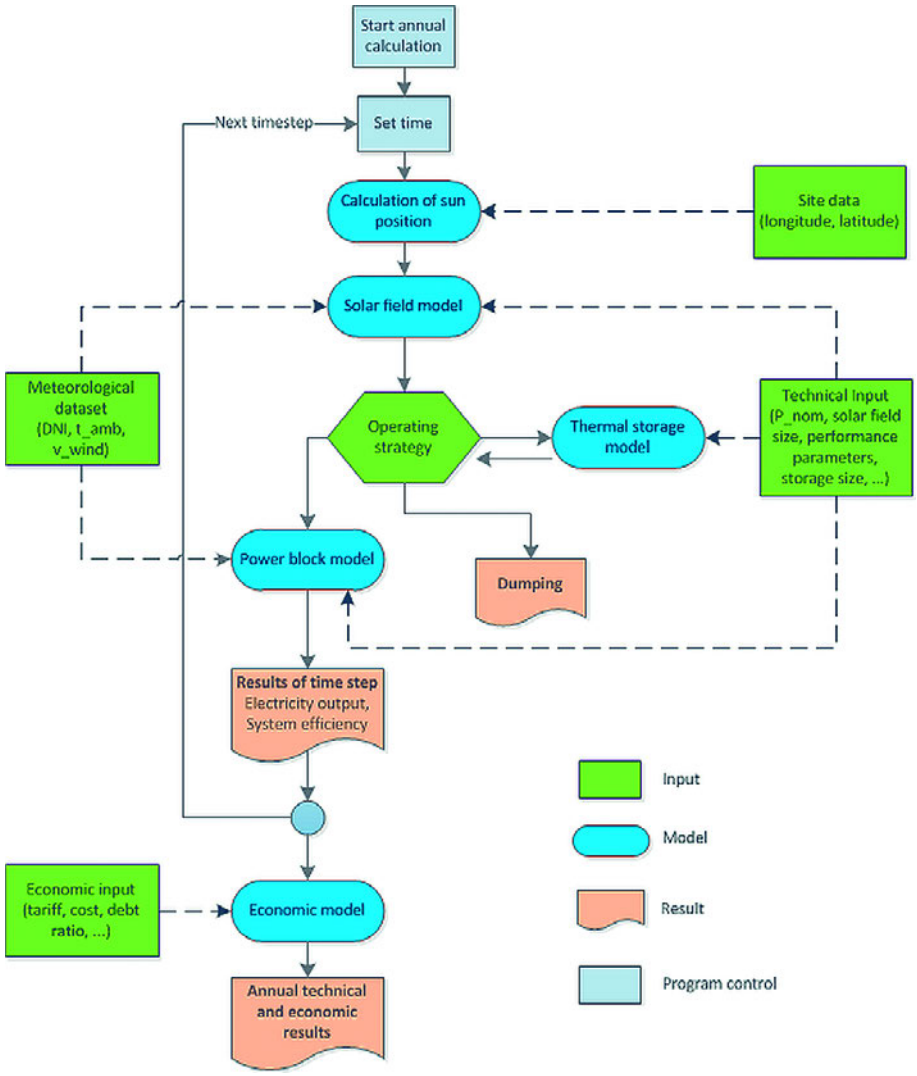

Figure 7: Simplified scheme of the CSP plant calculation in Greenius.

3.4 Economic viability

Having discussed in Section 3.3 the general differences between a solar only and a ToD specific operating strategy, now the impact of forecasts and nowcasts on the economic viability of these operating strategies is investigated. Real now- and forecasts are always affected by forecast errors and in the upcoming section their impact on the revenues under a ToD specific operating strategy are quantified. In a first step, the optimization potential and the optimization are checked by using different scenarios for the PSA site and the year 2013:

a) Solar only operating strategy (OS)

b) A fixed OS with the rule to fill the storage up to 50 % of its capacity every day prior to starting the power block, representing a simple OS which shifts the electricity production towards the evening hours.

c) An optimized OS as outlined in Section 3.3 using the day 1 ECMWF forecast

d) The same optimized OS using the ground observation based persistence forecast

e) The same optimized OS using the day 0 ECMWF forecast

f) The same optimized OS using the $DNI_{combined}$ from the available 3 months and the day 0 ECMWF forecast for the other 9 months

g) The same optimized OS using the ideal forecast

Electricity production between 22:00 and 5:00 is prohibited for all scenarios as there is no remuneration during this period (Fig. 6).

The second step is to apply scenarios c) to g) to different calendar years with varying meteorological conditions and the third step to check the impact of the site. This was done by applying the scenarios to the same CSP plant configuration, but assuming that they are located virtually either at PSA, Spain or at GHA, Algeria.

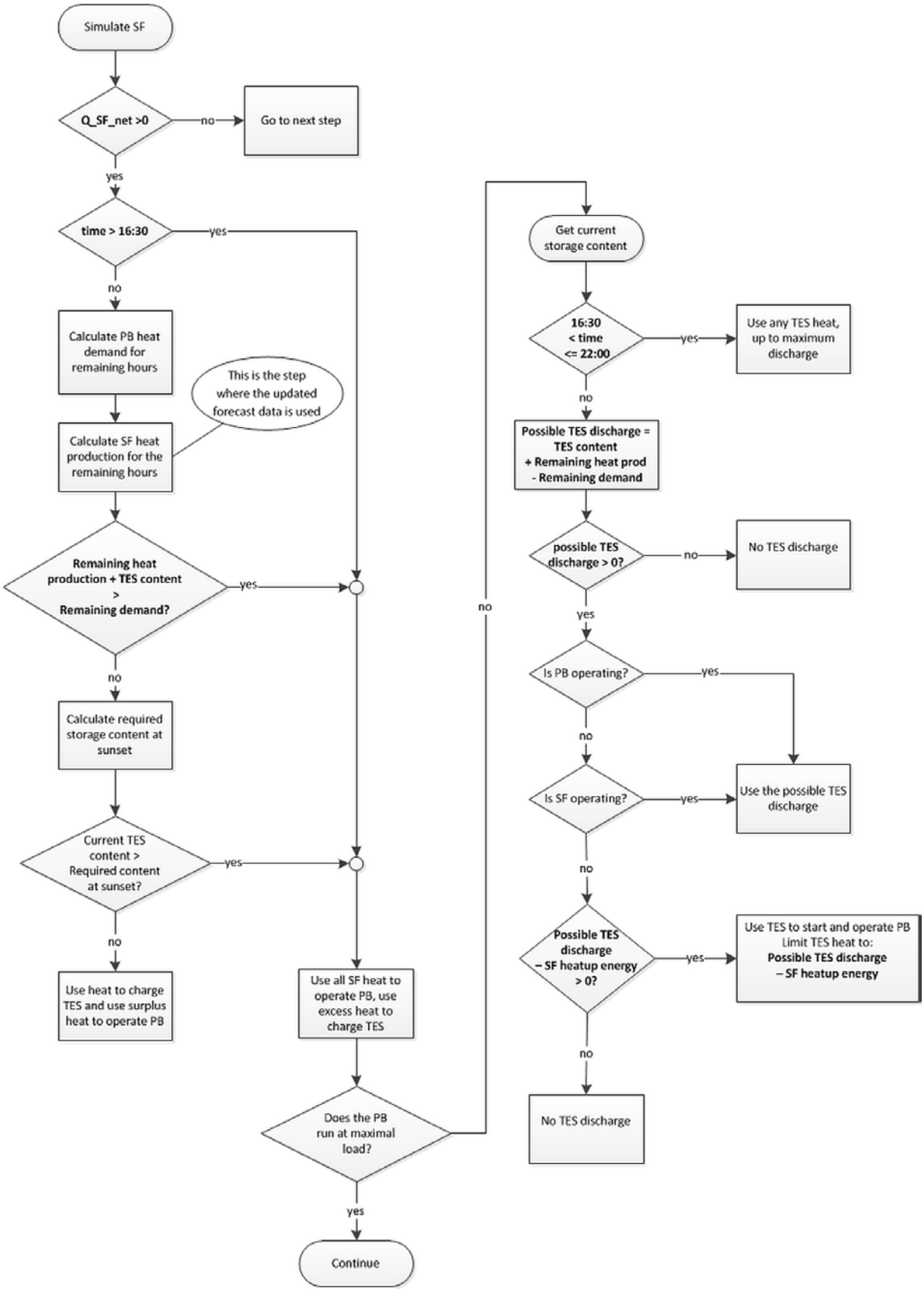

Figure 8: Flow-chart for the utilization of heat produced by the solar field (left) and for the decision about thermal storage discharging (right) in an operating strategy taking meteorological nowcasts into account. Abbreviations: SF, solar field; Q_SF_net, heat delivered by the solar field to the power block; PB, power block; TES, thermal energy storage.

Table 3: Annual sum of DNI for the different years and sites (measured on site) and a list of months for which DNIcombined is available in each year.

Site / Year	**PSA 2010**	**PSA 2013**	**PSA 2014**	**PSA 2015**	**GHA 2013**	**GHA 2014**
Annual DNI in kWh/m²	2094	2363	2425	2237	2396	2241
Months with available $DNI_{combined}$ forecast	Jan–Mar	Mar–May	Jun–Aug	Sep–Nov	Mar–May	Jun–Aug

Table 4: Results for the parabolic trough plant at PSA for 2013 under different scenarios.

Scenario	**W_{net} in GWh/a**	**Revenues in Mio. €**	**Rel. revenues**	**Dumping**
Optimized OS with ideal forecast	339,8	59.142	104,4 %	11,3 %
Optimized OS with DNI Combined forecast *)	338,1	57.789	102,1 %	11,6 %
Optimized OS with day 0 ECMWF forecast	338,1	57.392	101,4 %	11,6 %
Optimized OS with persistence forecast *)	338,8	57.257	101,1 %	11,5 %
Optimized OS with day 1 ECMWF forecast	331,1	56.623	100,0 %	13,5 %
Fixed OS (50% storage capacity)	329,5	54.163	95,7 %	13,4 %
Solar only OS	342,1	50.465	89,1 %	10,7 %

*) only 3 months March to May, for the other nine months ECMWF day 0 forecasts were used.

4 Results

Table 4 shows the results from the application of different scenarios at the PSA site for the year 2013 and for the parabolic trough power plant configuration. The maximum annual net electricity production (W_{net}) is reached for the solar only OS since this strategy gives the lowest dumping of heat which might be produced by the solar field but actually cannot be produced since there is no free power block or storage capacity. Applying the optimization with forecasts or even a simple fixed OS decreases the net electricity production as the actual solar heat production is reduced, but increases the annual revenues as it optimizes the production in terms of the ToD scheme. Results for the solar tower plant at PSA for 2013 are similar to those of the parabolic trough plant and the relative revenues are shown in Fig. 11, except for the solar only and fixed OS since they are of no practical relevance for a CSP plant with such a ToD scheme. They have been mentioned in Table 4 just to show the lower boundary and the impact of using any forecast scheme.

The scenario using the day 1 ECMWF forecast is set as a reference, as such forecasts are available from the day-ahead scheduling already at the power plant. For the reference case, the optimized OS using the ideal forecast gives about 4.4 % higher annual revenues while the solar only OS leads to almost 11 % lower revenues. These numbers show the relevance of such an optimization for serving the electricity market needs in such ToD tariff structures better. Furthermore, the dumping rate reached with the ideal forecast is only slightly higher than the optimal dumping rate as obtained in the solar only OS. This is interpreted as indication that the result of using a very good forecast in an OS is economically optimized, but also at least close to the overall possible technical potential of solar production in such a power plant.

As an illustrative example, Fig. 9 plots input data and results for the solar tower plant on a single day with varying DNI. The receiver heat output follows more or less the DNI and is the same in all 4 figures. The tariff is shown in orange and is also identical. Differences are in the electrical output and the dumping. Operation under the solar only OS shows no dumping for this day, but it is also obvious that no electricity is produced during high tariff hours. Optimized OS with the ECMWF day 0 forecast shifts the production towards the high tariff hours, but also shows some dumping after 12:00. The thermal storage is totally charged at this time and the solar field delivers more heat than the power block can utilize. Compared to this the optimized OS based on the $DNI_{combined}$ shows less dumping and more electricity production during the high tariff hours. Finally, the optimized OS based on the ideal forecast shows the highest electricity production during high tariff hours. Dumping is almost the same as in the $DNI_{combined}$ case.

These plots can be drawn also for other days and as one would expect, the differences between the scenarios are generally more pronounced for days with varying DNI. Clear sky conditions are easier to handle, provided that the forecast does predict them correctly. Fig. 9 shows that the simulation predicts several power block starts and shutdowns for the optimized OS during the day. This kind of operation is mainly caused by varying forecasts, but would not be favorable for a real plant. There is no penalty for this kind of on-off-operation included in the model. Since it occurs in almost all scenarios, the impact on the overall results is similar in all cases and we do not expect a significant impact on the calculated relative revenues.

Fig. 10 and Fig. 11 show the overall results for the yearly data sets for both types of CSP plants. Again, the optimized OS based on the ECMWF day 1 forecast is used as reference case. Using the ECMWF day 0 forecasts gives already higher revenues than using the day 1 forecast. The $DNI_{combined}$ forecast gives higher revenues than the other datasets for almost all cases

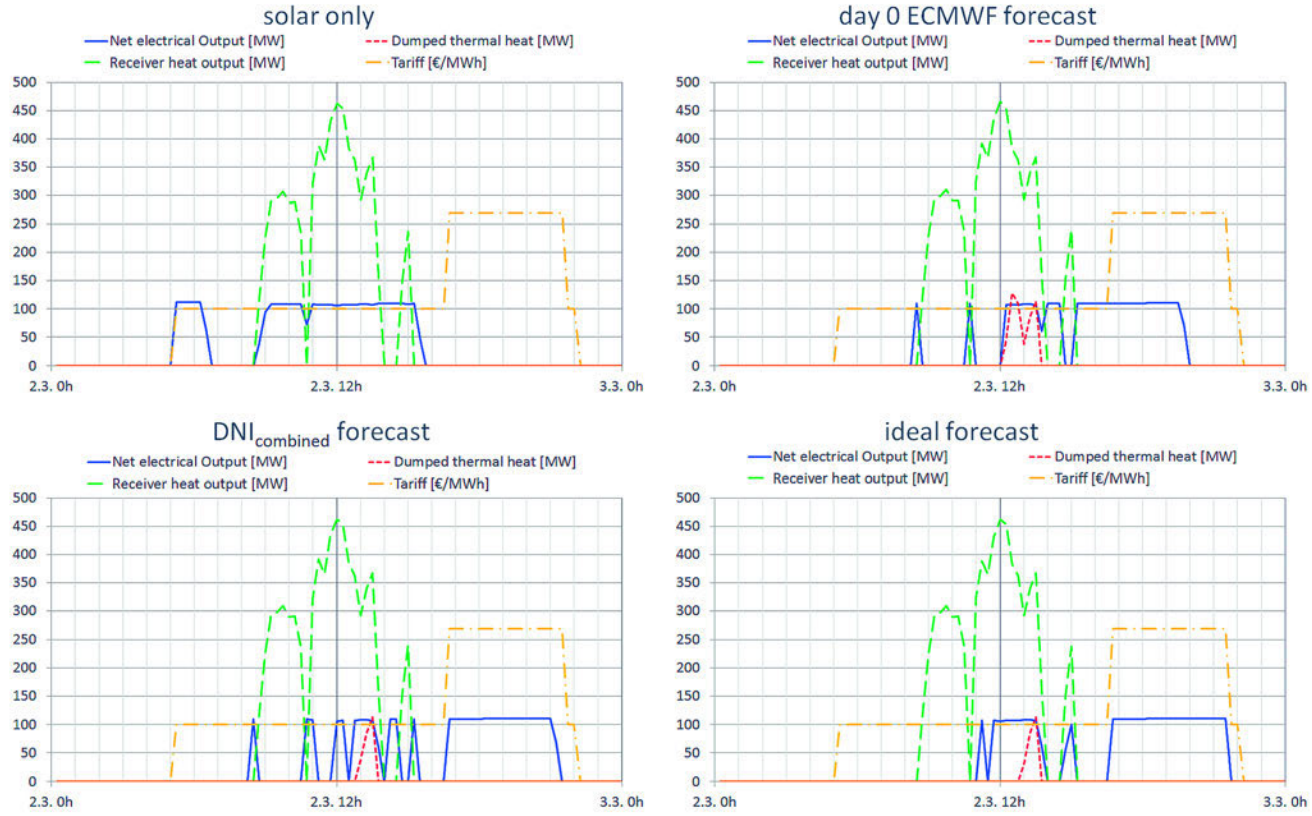

Figure 9: Detailed results for the solar tower plant at PSA for a single day in 2013.

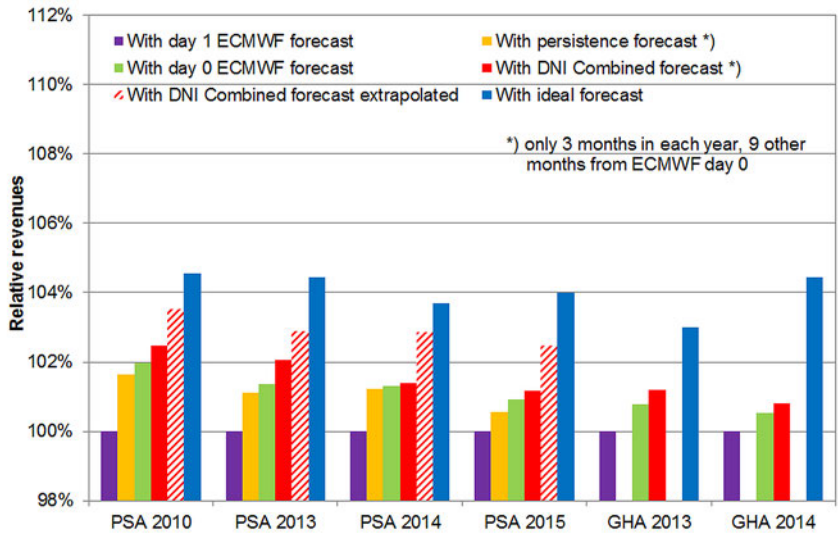

Figure 10: Relative annual revenues for the parabolic trough plant under different scenarios, for different years and sites (PSA: Plataforma Solar de Almeria, Spain; GHA: Ghardaia, Algeria).

except for the tower configuration at PSA in 2015. The results show that such an optimization makes sense and may increase the revenues significantly.

The actual benefit depends on the base line which is used as benchmark. If the ECMWF day ahead (day 1) forecast is used as benchmark, $DNI_{combined}$ forecasts increase the revenues by up to 4 % for the solar tower and up to 2 % for the parabolic trough plant. Comparing the results from the $DNI_{combined}$ forecast with those from the ECMWF day 0 forecast, one should keep in mind that these forecast datasets only differ for 3 months in each year. The remaining 9 months are identical. Therefore

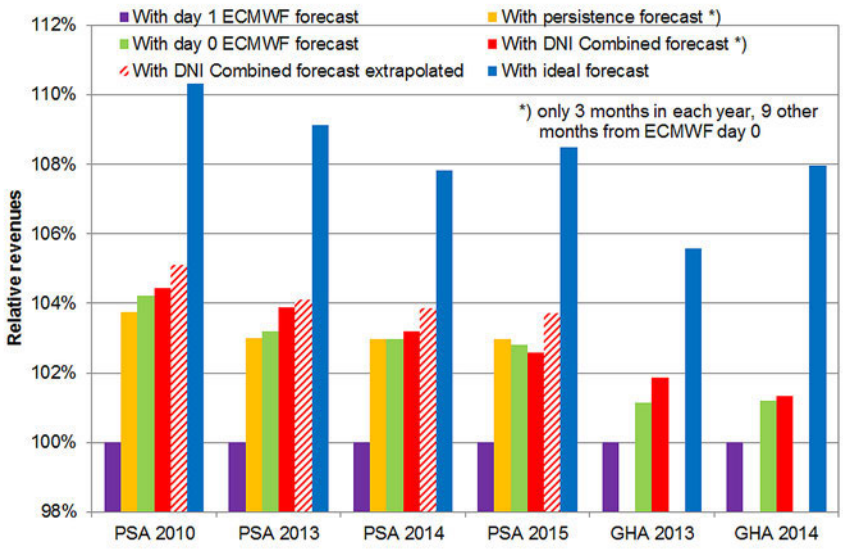

Figure 11: Relative annual revenues for the solar tower plant under different scenarios, for different years and sites (PSA: Plataforma Solar de Almeria, Spain; GHA: Ghardaia, Algeria).

one can expect a larger benefit if the $DNI_{combined}$ forecasts for the full year had been available.

The benefit with a 12 months data set can only be estimated roughly from the available data and is included for the PSA site in a separate column (red hachures to indicate extrapolation) called "$DNI_{Combined}$ forecast extrapolated". This column is generated by adding the differences in revenues between ECMWF day 0 and $DNI_{combined}$ forecast of the other 3 years to the actual one. Each PSA $DNI_{combined}$ dataset contains 3 different months of nowcasting data, only March is mentioned twice in 2010 and 2013 and December is missing. Therefore, the extrapolation implies that the benefit for 2010 for the months March to May will the same as for 2013, for June to August will be the same as for 2014, etc. This is of course just a rough extrapolation but may be used as first indicative value for a full year. Applying the same extrapolation to the persistence forecast would lead to even lower values than those shown as yellow columns in Fig. 10 and Fig. 11.

According to the tariff scheme used here, one percent of additional revenues correspond to an absolute amount of 570,000 EUR per year for the trough technology and of 660,000 EUR per year for the tower technology in the chosen technical specification of a 110 MW CSP power plant. The use of a nowcast scheme therefore creates additional revenues of up to 450,000 to 2,900,000 Euros per year for a 110 MW CSP plant in our study – dependent on the location and calendar year. This amount may be earned when an updated optimized forecast based on nowadays state-of-the-art in the meteorological community is used to adapt the operating strategy to maximize revenues. The values generated with the ideal forecast may be used to estimate the maximum economic potential of using forecasts.

It was found that the benefit of using forecasts is nearly twice as high for solar tower plants compared to troughs. The explanation for this difference is due to the different storage technology used in the parabolic trough and the solar tower plants. Both are using 2-tank molten salt thermal storage, but the solar tower uses molten salt also as heat transfer fluid (direct storage). The tower plant takes liquid salt from the cold storage, heats it up at the receiver and stores in in the hot salt tank. The parabolic trough plant uses thermal oil as heat transfer fluid and needs heat exchangers for charging and discharging the storage (indirect storage). The heat exchangers are causing a temperature drop, thus in storage discharging mode the temperature and the thermal input to the power block are reduced compared to the direct utilization of the heat collected by the solar field. Shifting heat from day time hours to evening hours is less efficient for the parabolic trough plant and therefore the revenue gain potential is smaller.

The impact of the DNI resource quantified as annual sum of DNI on the optimization potential cannot be assessed fully as the number of years and stations is very restricted due to the sparse public DNI ground measurement availability. Generally, it is expected that an optimization is much easier for clear sky days and they will occur more frequently during years with higher annual DNI. This expected behavior is confirmed in our study by the tendency showing a higher optimization potential (represented by the ideal forecast column) for years with lower DNI if looking at both sites separately. For PSA the 2010 dataset has the lowest annual sum of DNI and the 2014 dataset has the highest annual sum of DNI. For GHA the 2013 dataset has a higher annual sum of DNI than the 2014 dataset. Nevertheless, it is recommended to investigate further locations and multi-annual full year datasets to confirm this tendency.

5 Conclusions

Using frequently updated DNI nowcasts for CSP power plants may maximize their revenues under certain tariff conditions. Such tariff conditions support power plants with storage capabilities being able to provide electricity during evening peak demand hours even after sunset. Thermal storage may be used to shift production from daytime to low sun or night conditions, but filling the storage too early may cause losses as available sunlight cannot be used anymore as typically the full solar yield of a CSP power plant with storage is larger than the direct feed-in to the turbine and electricity grid allows.

Nowadays, CSP power plants already use day-ahead forecasts based on numerical weather predictions and therefore, they have routinely access to the first 3 to 5 days of forecasts from a numerical weather prediction model. The study investigates the impact economic value of adding a nowcasting component to the existing forecast tools.

The theoretical potential impact of a nowcasting scheme was quantified in order to understand if a nowcasting scheme adds value at all to nowadays used solar forecasting schemes for the day-ahead electricity market participation. The potential for this maximization is higher for solar tower plants with up to 10.3 % due to their direct storage technology compared to the value of up to 4.5 % for parabolic trough power plants using indirect molten salt storage.

Furthermore, this paper makes use of outcomes originating from a research project providing a large variety of nowadays state-of-the-art meteorological nowcasting methods from the research community. These rely on ground observations, satellites, and numerical weather prediction. Several well-known meteorological approaches were investigated with the focus of solar production nowcasting as a new application. These approaches include various combinations of optical flow motion vector tracking from satellite remote sensing, separate treatment of thin ice and other clouds in cloud retrievals, cloud object detection and tracking, cloud index and cloud optical thickness assessment, mesoscale wind field as well as radiation modeling, data assimilation, and radiative transfer methods. In order to derive a best-of approach, a merger was developed taking uncertainties into account as known for various time horizons and regions based on historical assessments or as online estimate provided in the nowcast method itself.

It could be shown that the $DNI_{combined}$ forecast as outcome of this merger procedure leads to higher revenues compared to the currently used day-ahead forecasts as e.g. from the ECMWF IFS in almost all cases investigated here. An annual benefit between 0.8 and 4.4 % compared to the day 1 ECMWF forecast is found. This implies an economical advantage of up to 2.9 Mio EUR of additional annual revenues of a typical 110 MW power plant. The study concludes that this economic impact is likely achievable by operational and commercial forecast providers based on the nowadays scientific state of the art.

Note that the study does not claim that exactly this merger method of all the various input nowcasts is the economical optimum with respect to costs of meteorological service providers. One may find a subset of a few of approaches sufficient. But the evaluation of Dubranna and Saint-Drenan (2017) also showed that there is no single nowcast strategy performing best overall forecast horizons and even at the same forecast horizon, the accuracy of the nowcast was depending very much on the location. So, the approach of combining a group of nowcasts in a merger strategy as presented here is recommended – without claiming that the choice as done in the DNICast project is the optimum solution.

The available nowcasting datasets were restricted to three months within four different years due to the high computer effort to generate some of the nowcasting approaches – namely the assimilation experiments and mesoscale ensemble modeling of a large area covering half of Spain required large computing facilities as they have not been further optimized numerically yet. For the study, the economic benefit was therefore extrapolated to whole years based on the results for 3 months. In a next step full years should be considered in order to confirm the extrapolated impact range.

There is still potential for improvement for all nowcast datasets, as shown by the comparison with the ideal forecast derived from ground observations as the truth.

Acknowledgement

The results published here are part of the DNICast project which has received funding from the European Union's Seventh Programme for research, technological development and demonstration under the agreement No [608623]. We thank ECMWF for providing historical forecasts from their IFS system. We would also like to thank CDER (Centre de Développement des Energies Renouvelables) for maintaining the meteorological station in Ghardaia and the colleagues at the Plataforma Solar de Almeria for maintaining the facility.

Acronyms and definitions

BSRN	Baseline Surface Radiation Network
CSP	Concentrating solar power, thermal power plants using concentrated sunlight as heat source to generate electricity
DNI	Direct normal irradiance. Part of the radiation that is received from the direction of the sun by a plane facing the sun.
ECMWF	European Centre for Medium-Range Weather Forecasts
EU FP7	7th Framework Programme of the European Union

GHA	Ghardaia, Site in Algeria
IFS	Integrated Forecast System as operated at the ECMWF
MENA	Middle East and Northern Africa
MESOR	Management and Exploitation of Solar Resource Knowledge, a 6th Framework Programm project on standardization
NWP	Numerical weather prediction
OS	Operating strategy for a CSP plant
PB	Power block
PSA	Plataforma Solar de Almeria, Site in Spain
PV	Photovoltaic
RMSE	Root mean square error
SF	Solar field
TES	Thermal energy storage
ToD	Time of delivery
UTC	Universal time code

Annex A

This annex summarizes the power plant technical configuration as used in this study.

Table 5: Table 5: Specifications of the parabolic trough oil plant.

Solar field		Unit
Collector type	Eurotrough 150	
Receiver	Schott PTR 70	
Number of collectors per loop	4	
Total number of loops	296	
Heat transfer fluid	Therminol VP-1	
Maximum bulk heat transfer fluid (HTF) temperature	393	°C
Power block		
Gross electric output	110	MW
Cooling type	Air cooled condenser	
Live steam temperature	383	°C
Live steam pressure	100	bar
Nominal gross efficiency	38.7	%
Thermal storage		
Storage type	2-tank indirect	
Storage Medium	Solar salt	
Net storage capacity	1420	MWh_{th}

Table 6: Specifications of the solar tower plant.

Solar field		Unit
Area of single heliostats	120	m^2
Total aperture area	1,014,429	m^2
Receiver	External cylindrical shape	
Heat transfer fluid	Solar salt	
Maximum bulk HTF temperature	565	°C
Power block		
Gross electric output	110	MW
Cooling type	Air cooled condenser	
Live steam temperature	540	°C
Live steam pressure	120	bar
Nominal gross efficiency	43.4	%
Thermal storage		
Storage type	2-tank direct	
Storage Medium	Solar salt	
Net storage capacity	1280	MWh_{th}

References

Bengtsson, L., U. Andrae, T. Aspelien, Y. Batrak, J. Calcvo, W. De Rooy, E. Gleeson, B. Hansen-Sass, M. Homleid, M. Hortal, K.-I. Ivarsson, G. Lenderink, S. Niemelä, K. Pagh Nielsen, J. Onvlee, L. Rontu, P. Samuelsson, D. Santos Munoz, A. Subias, S. Tijm, V. Toll, X. Yang, M. Odegaard Koltzow, 2017: The HARMONIE-AROME model configuration in the ALADIN-HIRLAM NWP system, – Mon. Wea. Rev. **145**, 1919–1935, DOI: 10.1175/MWR-D-16-0417.1.

Beyer, H.G., J.P. Martinez, M. Suri, J.L. Torres, E. Lorenz, C. Hoyer-Klick, P. Ineichen, 2008: MESOR project deliverable report D 1.1.1 Handbook on Benchmarking, Management and Exploitation of Solar Resource Knowledge. – MESOR CA – Contract No. 038665.

Bugliaro, L., T. Zinner, C. Keil, B. Mayer, R. Hollmann, M. Reuter, W. Thomas, 2011: Validation of cloud property retrievals with simulated satellite radiances: a case study for SEVIRI. – Atmos. Chem. Phys. **11**, 5603-5624, DOI: 10.5194/acp-11-5603-2011.

Chhatbar, K., R. Meyer, 2011: The influence of meteorological parameters on the energy yield of solar thermal power plants. – SolarPACES Conference, Granada, Spain.

Dersch, J., Dieckmann, S., 2015: Techno-Economic Evaluation of Renewable Energy Projects using the Software greenius. – Int. J. Thermal Env. Engineer. **10**, DOI: 10.5383/ijtee.10.01.003.

Dersch, J., K. Hennecke, V. Quaschning, 2010: Greenius – A Simulation Tool for Renewable Energy Utilization. – In: Proceedings of the SolarPACES 2010 Conference, 21.–24. September 2010, Perpignan, France.

Do Amaral Burghi, A.C., T. Hirsch, R. Pitz-Paal, 2017: CSP Dispatch Optimization Considering Forecast Uncertainties. – SolarPACES conference 2017, Santiago, Chile.

Dubranna, J., Y.M. Saint-Drenan, 2017: Validation of nowcasted DNI methods, Deliverable D4.3. – DNICast project, http://www.dnicast-project.net.

Gaston, M., T. Landelius, M. Schroedter-Homscheidt, C. Bergemann, 2017: Report on NWP variational assimilation, particle filtering, and machine learning approaches for short term DNI nowcasting, D3.11 deliverable report. – DNICast project, http://www.dnicast-project.net.

Gauché, P., J. Rudman, M. Mabaso, W.A. Landman, T.W. von Backström, A.C. Brent, 2017: System value and progress of CSP. – Sol. Energy **152**, 106–139, DOI: 10.1016/j.solener.2017.03.072.

Gesell, G., 1989: An Algorithm for Snow and Ice Detection Using AVHRR data: An Extension to the APOLLO Software Package. – Int. J. Rem. Sens. **10**, 897–905. DOI: 10.1080014311689089039 29.

Geuder, N., Wolfertstetter, F., Wilbert, S., Schüler, D., Affolter, R., Kraas, B., Lüpfert, E., Espinar, B., 2015. Screening and Flagging of Solar Irradiation and Ancillary Meteorological Data. – Energy Procedia **69**,1989–1998. DOI: 10.1016/j.egypro.2015.03.205.

Guedez, R., M. Topel, I. Conde, F. Ferragut, I. Callaba, J. Spellin, Z. Hassar, C.D. Perez-Segarra, B. Laumert, 2016: A Methodology for Determining Optimum Solar Tower Plant Configurations and Operating Strategies to Maximize Profits Based on Hourly Electricity Market Prices and Tariffs. – J. Sol. Energy Eng. **138**, DOI: 10.1115/1.4032244.

Hammer, A., E. Lorenz, A. Kemper, D. Heinemann, H.G. Beyer, K. Schumann, M. Schwandt, 2009: Direct Normal Irradiance for CSP based on satellite images of Meteosat Second Generation. – Proc. SolarPACES Symposium, Berlin (Germany), September 15–18, 2009

Ineichen, P., R. Perez, 2002: A new airmass independent formulation for the Linke turbidity coefficient. – Sol. Energy **73**, 151–157, DOI: 10.1016/S0038-092X(02)00045-2.

ISO 9060, 1990: Solar Energy – Specification and Classification of Instruments for Measuring Hemispherical Solar and Direct Solar Radiation. Standard of the International Organization for Standardization (ISO). – International Organization for Standardization.

Kos, S., L. Bugliaro, A. Ostler, 2014: Retrieval of cirrus cloud optical thickness and top altitude from geostationary remote sensing. – Atmos. Meas. Tech. **7**, 3233–3246, DOI: 10.5194/amt-7-3233-2014.

Kraas, B., M. Schroedter-Homscheidt, R. Madlener, 2013: Economic merits of a state-of-the-art concentrating solar power forecasting system for participation in the Spanish electricity market. – Sol. Energy **93**, 244–255, DOI: 10.1016/j.solener.2013.04.012.

Kriebel, K.T., Gesell, G., Kästner, M., Mannstein, H., 2003: The cloud analysis tool APOLLO: Improvements and Validation. – Int. J. Rem. Sens., **24**, 2389-2408, DOI: 10.1080/01431160210163065.

Kriebel, K.T., R.W. Saunders, G. Gesell, 1989: Optical Properties of Clouds Derived from Fully Cloudy AVHRR Pixels. – Beitr. Phys. Atmos. **62**, 165–171.

Landelius, T., M. Lindskog, S. Müller, T. Sirch, 2016: Report on satellite-based nowcasting methods, D3.6 deliverable report. – DNICast projct, http://www.dnicast-project.net.

Le Gleau, H., M. Derrien, 2002: 'User manual for the PGE01-02-03 of the SAFNWC/MSG: Scientific part', EUMETSAT documentation SAF NWC/IOP/MFL/SCI/SUM/01. – Centre de Meteorologie Spatiale: Toulouse, France.

Long, C.N., E.G. Dutton, 2012: BSRN Global Network recommended QC tests, V2.0. – http://www.bsrn.awi.de/fileadmin/user_upload/Home/Publications/BSRN_recommended_QC_tests_V2.pdf.

Lovegrove, K., G. James, D. Leitch, A. Milczarek, A.J. Ngo, M. Rutovitz, M. Watt, J. Wyder, 2018: Comparison of dispatchable renewable electricity options, ARENA. – https://www.solarpaces.org/wp-content/uploads/Comparison-of-Dispatchable-Renewable-Energy-Options-Technologies-for-an-Orderly-Transition.pdf

Merk, D., T. Zinner, 2013: Detection of convective initiation using Meteosat SEVIRI. implementation in and verifcation with the tracking and nowcasting algorithm Cb-TRAM. – Atmos. Meas. Tech. **6**, 1903-1918, DOI: 10.5194/amt-6-1903-2013.

Meyer, R., N. Geuder, E. Lorenz, A. Hammer, H.G. Beyer, 2008: Combining solar irradiance measurements and various satellite-derived products to a site-specific best estimate. – In: SolarPACES Conference 4–7 March 2008, Las Vegas, USA, 1–8.

Rigollier, C., M. Lefevre, L. Wald, 2004: The method Heliosat-2 for deriving shortwave solar radiation data from satellite images. – Sol. Energy **77**, 2, 159-169, DOI: 10.1016/j.solener.2004.04.017.

Saunders, R.W., K.T. Kriebel, 1988: An improved method for detecting clear sky and cloudy radiances from AVHRR data.- Int. J. Rem. Sens. **9**, 123–150, DOI:10.1080/01431168808954841.

Schroedter-Homscheidt, M., C. Hoyer-Klick, E. Rikos, S. Tselepsis, B. Pulvermüller, 2009: Nowcasting and Forecasting of Solar Irradiance for Solar Energy Electricity Grid Integration. – Proceedings, 33rd International Symposium on Remote Sensing of Environment, ISRSE. 4.–8. Mai 2009, Stresa, Italien, https://elib.dlr.de/58994.

Schroedter-Homscheidt, M., G. Gesell, 2016: Verification of sectoral cloud motion based direct normal irradiance nowcasting from satellite imagery. – SolarPaces Conference, AIP Conference Proceedings, 2734, 150007, DOI: 10.1063/1.4949239.

Schroedter-Homscheidt, M., B. Pulvermüller, 2011: Verification of direct normal irradiance forecasts for the concentrating solar thermal power plant Andasol-3 location. – In: Proceedings. SolarPaces 2011, 20.-23. September 2011, Granada, Spanien, http://elib.dlr.de/74331.

Schüler, D., S. Wilbert, N. Geuder, R. Affolter, F. Wolfertstetter, C. Prahl, M. Röger, M. Schroedter-Homscheidt, G. Abdellatif, A. Allah Guizani, M. Balghouthi, A. Khalil, A. Mezrhab, A. Al-Salaymeh, N. Yassaa, F. Chellali, D. Draou, P. Blanc, J. Dubranna, O.M. K. Sabry, 2016: The enerMENA meteorological network – Solar radiation measurements in the MENA region. - AIP Conference Proceedings, 1734 (1), 150008, DOI: 10.1063/1.4949240.

Sirch, T., L. Bugliaro, T. Zinner, M. Möhrlein, M. Vazquez-Navarro, 2017: Cloud and DNI nowcasting with MSG/SEVIRI for the optimized operatio of concentrating solar power plants. – Atmos. Meas. Tech. **10**, 2, 409–429, DOI: 10.5194/amt-10-409-2017.

Van der Veen, S.H., 2013: Improving NWP Model Cloud Forecasts Using Meteosat Second-Generation Imagery. – Mon. Wea. Rev. **141**, 1545–1557, DOI: 10.1175/MWR-D-12-00021.1.

Vasallo, M.J., J.M. Bravo, 2016: A novel two-model based approach for optimal scheduling in CSP plants. – Sol. Energy **126**, 73–92, DOI: 10.1016/j.solener.2015.12.041.

Wagner, M.J., A.M. Newman, W.T. Hamilton, R.J. Braun, 2017: Optimized dispatch in a first-principles concentrating solar power production model. – Appl. Energy **203**, 959–971, DOI: 10.1016/j.apenergy.2017.06.072.

Wey, E., M. Schroedter-Homscheidt, 2014: APOLLO Cloud Product Statistics. – Energy Procedia **49**, 2414–2421, DOI: 10.1016/j.egypro.2014.03.256.

Wilbert, S., B. Reinhardt, J. Devore, M. Röger, R. Pitz-Paal, C. Gueymard, R. Buras, 2013: Measurement of Solar Radiance Profiles With the Sun and Aureole Measurement System. – J. Solar Energy Engineer. **35**, 041002-041002, DOI: 10.1115/1.4024244.

Wittmann, M., M. Eck, R. Pitz-Paal, H. Müller-Steinhagen, 2011: Methodology for optimized operation strategies of solar thermal power plants with inte-

grated heat storage. – Sol. Energy **85**, 4, 653–659, DOI: 10.1016/j.solener.2010.11.024.

Zinner, T., H. Mannstein, A. Tafferner, 2008: Cb-TRAM: Tracking and monitoring severe convection from onset over rapid development to mature phase using multi-channel Meteosat-8 SEVIRI data. – Meteor. Atmos. Phys. **101**, 191–2010, DOI: 10.1007/s00703-008-0290-y.

Zinner, T., C. Forster, E. De Conging, H.-D. Betz, 2013: Validation of the Meteosat storm detection nd nowcasting system Cb-TRAM with ligthning network data – Europe and South Africa. – Atmos. Meas. Tech. **6**,1567–1583, DOI: 10.5194/amt-6-1567-2013.